

# Muon anomaly and a lower bound on higgs mass due to a light stabilized radion in the Randall-Sundrum model.

Prasanta Kumar Das <sup>1</sup>

Harish-Chandra Research Institute,  
Chhatnag Road, Jhusi,  
Allahabad-211019, India .

*presently at*

Institute of Mathematical Sciences  
C.I.T Campus, Taramani,  
Chennai-600113, India

## Abstract

*We investigate the Randall-Sundrum model with a light stabilized radion (required to fix the size of the extra dimension) in the light of muon anomalous magnetic moment  $a_\mu [= \frac{g-2}{2}]$ . Using the recent data (obtained from the E821 experiment of the BNL collaboration) which differs by  $2.6 \sigma$  from the Standard Model result, we obtain constraints on radion mass  $m_\phi$  and radion vev  $\langle \phi \rangle$ . In the presence of a radion the beta functions  $\beta(\lambda)$  and  $\beta(g_t)$  of higgs quartic coupling ( $\lambda$ ) and top-Yukawa coupling ( $g_t$ ) gets modified. We find these modified beta functions. Using these beta functions together with the anomaly constrained  $m_\phi$  and  $\langle \phi \rangle$ , we obtain lower bound on higgs mass  $m_h$ . We compare our result with the present LEP2 bound on  $m_h$ .*

*Keywords:* Extra dimensional field theory; Renormalization; Higgs boson.

*PACS Nos.:* 11.10.Kk, 11.10.Gh, 14.80.Bn

---

<sup>1</sup>Email:pdas@mri.ernet.in, dasp@imsc.res.in

# 1 Introduction

Recently the notion of extra spatial dimension(s) [1, 2, 3, 4], proposed as a resolution of the hierarchy problem, draws a lot of attention among the physics community. Among these the Randall-Sundrum(RS) model (of warped spatial dimension) is particularly interesting from the phenomenological point of view[5, 6, 7, 8]. This model views the world as 5-dimensional and its fifth spatial dimension is  $S^1/Z_2$  orbifold. The metric of such a world can be written as

$$ds^2 = \Omega^2 \eta_{\mu\nu} dx^\mu dx^\nu - R_c^2 d\theta^2. \quad (1)$$

The factor  $\Omega^2 = e^{-2kR_c|\theta|}$  is called the warp factor. In  $\Omega^2$ ,  $k$  stands for the bulk curvature constant and  $R_c$  corresponds to the size of the extra dimension. The angular variable  $\theta$  parametrizes the fifth dimension. The model is constructed out of two  $D_3$  branes located at the orbifold fixed points.  $\theta = 0$  and  $\theta = \pi$  respectively. The brane located at  $\theta = 0$  (where gravity peaks) is known as the Planck brane, while that located at  $\theta = \pi$  (the SM fields resides on it and the gravity is weak) is called the TeV brane.

The radius  $R_c$ (distance between two branes) can be related to the vacuum expectation value (vev) of some modulus field  $T(x)$  which corresponds to the fluctuations of the metric over the background geometry given by  $R_c$ . Replacing  $R_c$  by  $T(x)$  we can rewrite the RS metric at the orbifold point  $\theta = \pi$  as

$$ds^2 = g_{\mu\nu}^{vis} dx^\mu dx^\nu, \quad (2)$$

where  $g_{\mu\nu}^{vis} = e^{-2\pi kT(x)} \eta_{\mu\nu} = \left(\frac{\phi(x)}{f}\right)^2 \eta_{\mu\nu}$ . Here  $f^2 = \frac{24M_5^3}{K}$ ,  $M_5$  is the 5-dimensional Planck scale [3, 4] and  $\phi(x) = f e^{-\pi kT(x)}$ . The scalar field  $\hat{\phi}(x)$  (i.e.  $\hat{\phi}(x) = \phi(x) - \langle\phi\rangle$ ) is known as the radion field [9, 10, 11]. In the minimal version of the RS model there is no potential which can stabilize the modulus field  $T(x)$  (and thus the radion  $\hat{\phi}(x)$ ). However in a pioneering work Goldberger and Wise [12, 13] were able to generate a potential of this modulus field (by adding an extra massive bulk scalar) field which has the correct minima satisfying  $kR_c \simeq 11$ , a necessary condition for the hierarchy resolution.

In this non-minimal RS model (RS model together with the Goldberger and Wise mechanism), the stabilized radion can be lighter than the other low-lying gravitonic degrees of

freedom and will reveal itself first either in the direct collider search or indirectly through the precision measurement. Studies based on observable consequences of radion are available in the literature [14, 15, 16, 17, 18, 19, 20]. Here we will make one such study in the light of muon anomalous magnetic moment  $a_\mu = \frac{g-2}{2}$ .

The E821 experiment [21, 22] of the BNL collaboration recently has reported a new measurement of muon magnetic moment ( $a_\mu^{(expt)}$ ) which is a positive one and deviates from the SM based calculation by  $2.6 \sigma$ . The measured experimental value  $a_\mu^{(exp)}$  lies in the range

$$a_\mu^{(expt)} = (11659204(7)(4)) \times 10^{-10} \quad (3)$$

in units of Bohr magneton  $e/2m_\mu$ . Comparing this and the present SM result (which includes QED, electroweak and hadronic contribution) [23, 24, 25, 26, 27] which is about

$$a_\mu^{(SM)} = (11659176 \pm 6.7) \times 10^{-10}, \quad (4)$$

one finds a lot of option to explain the extra contribution  $\delta a_\mu^{new} [= a_\mu^{(expt)} - a_\mu^{(SM)}]$  by means of some non-standard new physics [28, 29, 30, 31, 32, 33, 34, 35, 36, 37, 38, 39, 40, 41, 42, 43, 44, 46, 47]. At the same time by taking a conservative viewpoint one can also constrain the new physics by using this  $\delta a_\mu^{new}$ .

The organization of the paper is as follows. In section 2, we describe the effective interaction of radion and the SM fields (on the TeV brane). We obtain the effective renormalized higgs quartic and top-Yukawa couplings  $\lambda$  and  $g_t$  in the presence of radion and find the corresponding modified beta functions  $\beta(\lambda)$  and  $\beta(g_t)$ . We find the radion contribution to muon anomalous magnetic moment  $a_\mu^\phi$ . Section 3 is devoted for the numerical analysis. Defining the excess  $\delta a_\mu^{new} [= a_\mu^{(expt)} - a_\mu^{(SM)}]$  in terms of  $a_\mu^\phi$  (the radion contribution), we obtain constraints on radion mass  $m_\phi$  and radion vev  $\langle \phi \rangle$  which are the two free parameters of this model. Using these anomaly constrained  $m_\phi$  and  $\langle \phi \rangle$  and the modified beta functions  $\beta(\lambda)$  and  $\beta(g_t)$  we then obtain lower bounds on the SM higgs mass  $m_h$ . We compare our result with the LEP2 bound on  $m_h$  obtained from the direct search [48]. Finally we summarize our results and conclude.

## 2 Effective Interactions and Renormalization

Radion interaction with the SM fields(residing on the TeV brane) is governed by the 4 dimensional general coordinate invariance. It couples to the trace of the energy-momentum tensor of the SM fields as

$$\mathcal{L}_{int} = \frac{\hat{\phi}}{\langle\phi\rangle} T_{\mu}^{\mu}(SM), \quad (5)$$

where  $\langle\phi\rangle$  is the radion vev and  $T_{\mu}^{\mu}(SM)$  is given by

$$T_{\mu}^{\mu}(SM) = \sum_{\psi} \left[ \frac{3i}{2} (\bar{\psi}\gamma_{\mu}\partial_{\nu}\psi - \partial_{\nu}\bar{\psi}\gamma_{\mu}\psi) \eta^{\mu\nu} - 4m_{\psi}\bar{\psi}\psi \right] - 2m_W^2 W_{\mu}^{+}W^{-\mu} - m_Z^2 Z_{\mu}Z^{\mu} + (2m_h^2 h^2 - \partial_{\mu}h\partial^{\mu}h) + \dots \quad (6)$$

Note that in order to accommodate the gauge interaction(s) with fermion-radion system one has to write the ordinary derivative to a gauge covariant derivative. The photon and the gluons couple to the radion via the usual top-loop diagrams[49]. Besides this there is an added source of enhancement of the coupling due to the trace anomaly term (See [50] for a nice discussion) which is given by

$$T_{\mu}^{\mu}(SM)^{anom} = \sum_a \frac{\beta_a(g_a)}{2g_a} G_{\mu\nu}^a G^{a\mu\nu}. \quad (7)$$

For gluons  $\beta_s(g_s)/2g_s = -[\alpha_s/8\pi] b_{QCD}$  where  $b_{QCD} = 11 - 2n_f/3$  and  $n_f$  is the number of quark flavours. In the next subsection we derive in detail the radion interaction with the higgs scalar and the top quark as they will be relevant in our course of finding renormalized  $\lambda$  and  $g_t$ .

### 2.1 Radion-higgs coupling and $\lambda$ renormalization

The radion coupling to the higgs scalar is completely determined by 4 dimensional general covariance. The action for the higgs scalar in the Randall-Sundrum model can be written as

$$S = \int d^4x \sqrt{-g_{vis}} [g_{vis}^{\mu\nu} \frac{1}{2} \partial_{\mu}h\partial_{\nu}h - V(h)], \quad (8)$$

where  $V(h) = \frac{1}{2}\mu^2 h^2 + \frac{\lambda}{4}h^4$ .  $h$  is a small fluctuation of the higgs field from its classical vacuum  $v$ . In absence of graviton fluctuations we have  $g_{vis}^{\mu\nu} = e^{2k\pi T(x)}\eta^{\mu\nu} = \left(\frac{\phi}{f}\right)^{-2}\eta^{\mu\nu}$  and

$\sqrt{-g_{vis}} = \left(\frac{\phi}{f}\right)^4$  where  $\phi = f e^{-k\pi T(x)} = \langle\phi\rangle + \hat{\phi}$ . Rescaling  $h$  and  $v$  as  $h \rightarrow \frac{f}{\langle\phi\rangle}h$  and  $v \rightarrow \frac{f}{\langle\phi\rangle}v$  we get

$$S = \int d^4x \left[ \left(1 + \frac{\hat{\phi}}{\langle\phi\rangle}\right)^2 \frac{1}{2} \eta^{\mu\nu} \partial_\mu h \partial_\nu h - \left(1 + \frac{\hat{\phi}}{\langle\phi\rangle}\right)^4 V(h) \right], \quad (9)$$

where  $V(h) = \frac{\lambda}{4}(h^4 + 4h^3v + 4h^2v^2)$ .

The Feynman diagrams that give rise to the radion (in figures  $\phi \equiv \hat{\phi}$ ) contribution to the renormalization of the four higgs vertex in the RS model are shown in Figure 1a.

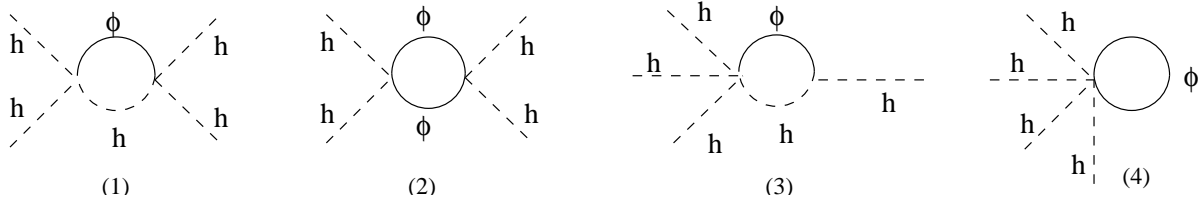


Figure 1a: Feynman diagrams that give rise to the radion contribution to the vertex renormalization. Here  $\phi$  corresponds to  $\hat{\phi}$ .

We now evaluate the vertex renormalization diagrams explicitly with a cut off  $\Lambda$  and the leading log terms of these diagrams are given by

$$\Gamma_1 = 6\lambda \frac{288\lambda v^2}{16\pi^2 \langle\phi\rangle^2} \ln \frac{\Lambda^2}{\mu^2}, \quad (10)$$

$$\Gamma_2 = 6\lambda \frac{144\lambda v^4}{16\pi^2 \langle\phi\rangle^4} \ln \frac{\Lambda^2}{\mu^2}, \quad (11)$$

$$\Gamma_3 = 6\lambda \frac{128\lambda v^2}{16\pi^2 \langle\phi\rangle^2} \ln \frac{\Lambda^2}{\mu^2}, \quad (12)$$

and

$$\Gamma_4 = -6\lambda \frac{6}{16\pi^2 \langle\phi\rangle^2} \left[ \Lambda^2 - m_\phi^2 \ln \frac{\Lambda^2}{\mu^2} \right]. \quad (13)$$

Here  $\mu$  is the renormalization scale. In the SM model the wavefunction renormalization constant of the higgs boson  $Z_h$  is equal to one at one loop order even after the higgs field

is shifted by its vev. However the radion coupling to the KE term of the higgs boson gives rise to a non-trivial wavefunction renormalization of the higgs boson. Evaluating the radion mediated self energy diagram (Figure 1b) of the higgs boson and considering the terms proportional to  $p^2$  we find that  $Z_h = 1 + \frac{1}{32\pi^2} \frac{5m_h^2 - m_\phi^2}{\langle\phi\rangle^2} \ln \frac{\Lambda^2}{\mu^2}$ .

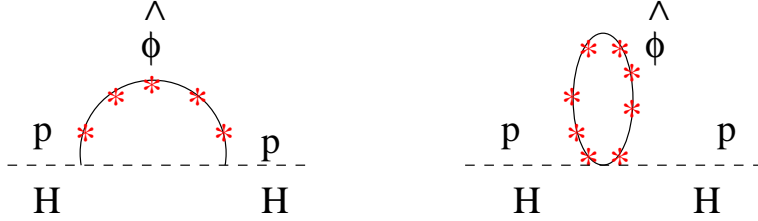


Figure 1b: Radion mediated self-energy diagram of the higgs boson.

Using the above vertex and wavefunction renormalizations induced by a light radion it can be shown that the complete one loop beta function for  $\lambda$  in the RS model is given by [51]

$$\beta(\lambda) = \mu \frac{d\lambda}{d\mu} = \frac{1}{8\pi^2} \left[ 9\lambda^2 + \frac{402\lambda^2 v^2}{\langle\phi\rangle^2} + \frac{144\lambda^2 v^4}{\langle\phi\rangle^4} + \frac{5\lambda m_\phi^2}{\langle\phi\rangle^2} + \lambda \left( 6g_y^2 - \frac{9}{2}g^2 - \frac{3}{2}g'^2 \right) \right] + \frac{1}{8\pi^2} \left[ -6g_y^4 + \frac{3}{16}(g^4 + \frac{1}{2}(g^2 + g'^2)^2) \right]. \quad (14)$$

The purely SM contribution to  $\beta(\lambda)$  (see the next subsection) can be obtained by letting the expansion parameter  $\langle\phi\rangle$  approach infinity.

## 2.2 Radion-top coupling and $g_t$ renormalization

The radion coupling to the top quark in the Randall-Sundrum model can be derived from the following action

$$S_1 = \int d^4x \sqrt{-g_v} \left[ \bar{\psi} (i\gamma_a e^{a\mu} D_\mu - m) \psi - \frac{g_t}{\sqrt{2}} H \bar{\psi} \psi \right], \quad (15)$$

where  $e^{a\mu}$  is the contravariant vierbein field for the visible brane. In the presence of radion fluctuation it satisfies the normalization condition

$$e^{a\mu} e_a^\nu = g^{\mu\nu} = \left( \frac{\phi}{f} \right)^{-2} \eta^{\mu\nu} = e^{2\pi k T(x)} \eta^{\mu\nu}. \quad (16)$$

$D_\mu$  is the covariant derivative with respect to general coordinate transformation and is given by

$$D_\mu \psi = \partial_\mu \psi + \frac{1}{2} w_\mu^{ab} \Sigma_{ab} \psi. \quad (17)$$

Here  $\Sigma_{ab} = \frac{1}{4} [\gamma_a, \gamma_b]$ . The spin connection  $w_\mu^{ab}$  in terms of the vierbein fields reads as

$$w_\mu^{ab} = \frac{1}{2} e^{\nu a} (\partial_\mu e_\nu^b - \partial_\nu e_\mu^b) - \frac{1}{2} e^{\nu b} (\partial_\mu e_\nu^a - \partial_\nu e_\mu^a) - \frac{1}{2} e^{\rho a} e^{\sigma b} (\partial_\rho e_{\sigma c} - \partial_\sigma e_{\rho c}) e_\mu^c. \quad (18)$$

It can be shown that in the presence of radion fluctuations on the visible brane the spin connection is given by

$$w_\mu^{ab} = \frac{1}{\phi} \partial_\nu \phi [e^{\nu b} e_\mu^a - e^{\nu a} e_\mu^b]. \quad (19)$$

The covariant derivative of the fermion field becomes

$$D_\mu \psi = \partial_\mu \psi + \frac{1}{4\phi} \partial^\nu \phi [\gamma_\mu, \gamma_\nu] \psi, \quad (20)$$

where the  $\gamma_\mu$  are independent of space time coordinates. The action comprising radion coupling to the top quark finally can be written as

$$\begin{aligned} S_1 &= \int d^4x \left( \frac{\phi}{f} \right)^4 \left[ \left( \frac{\phi}{f} \right)^{-1} \bar{\psi} \{ i\gamma^\mu \partial_\mu + \frac{3i}{2\phi} \partial_\mu \phi \gamma^\mu \} \psi - m_t \bar{\psi} \psi - \frac{g_t}{\sqrt{2}} H \bar{\psi} \psi \right] \\ &= \int d^4x \left[ \bar{\tilde{\psi}} \{ i\gamma^\mu \partial_\mu \tilde{\psi} + \frac{3i}{2\phi} \partial_\mu \phi \gamma^\mu \tilde{\psi} \} \left( 1 + \frac{\hat{\phi}}{\langle \phi \rangle} \right)^3 - \left( \tilde{m}_t + \frac{g_t}{\sqrt{2}} \tilde{H} \right) \left( 1 + \frac{\hat{\phi}}{\langle \phi \rangle} \right)^4 \bar{\tilde{\psi}} \tilde{\psi} \right] \\ &= \int d^4x \left[ \bar{\tilde{\psi}} i\gamma^\mu \partial_\mu \tilde{\psi} - \tilde{m}_t \bar{\tilde{\psi}} \tilde{\psi} - \frac{g_t}{\sqrt{2}} \tilde{H} \bar{\tilde{\psi}} \tilde{\psi} \right] \\ &\quad + \int d^4x \left[ \frac{3i}{\langle \phi \rangle} \bar{\tilde{\psi}} \gamma^\mu \partial_\mu \tilde{\psi} \hat{\phi} + \frac{3i}{2\langle \phi \rangle} \bar{\tilde{\psi}} \gamma^\mu \tilde{\psi} \partial_\mu \hat{\phi} - 4 \left( \tilde{m}_t + \frac{g_t}{\sqrt{2}} \tilde{H} \right) \frac{\hat{\phi}}{\langle \phi \rangle} \bar{\tilde{\psi}} \tilde{\psi} \right] \\ &\quad + \int d^4x \left[ 3 \bar{\tilde{\psi}} i\gamma^\mu \partial_\mu \tilde{\psi} \frac{\hat{\phi}^2}{\langle \phi \rangle^2} + \frac{3i}{\langle \phi \rangle^2} \hat{\phi} \bar{\tilde{\psi}} \gamma^\mu \tilde{\psi} \partial_\mu \hat{\phi} - 6 \left( \tilde{m}_t + \frac{g_t}{\sqrt{2}} \tilde{H} \right) \frac{\hat{\phi}^2}{\langle \phi \rangle^2} \bar{\tilde{\psi}} \tilde{\psi} \right]. \quad (21) \end{aligned}$$

In above  $\psi = \left( \frac{f}{\langle \phi \rangle} \right)^{3/2} \tilde{\psi}$ ,  $H = \left( \frac{f}{\langle \phi \rangle} \right) \tilde{H}$  and  $m = \left( \frac{f}{\langle \phi \rangle} \right) \tilde{m}$ . In the following we shall assume that all fields and parameters have been properly scaled so as to corresponds to the TeV scale and drop the *tilde* sign.

We use the same cut-off regularization technique with the UV cut-off  $\Lambda$  for the following vertex renormalization diagrams (see Figure 2a) to determine the renormalized  $g_t$ . To find the contribution of these diagrams to  $H \bar{\psi} \psi$  vertex we have to consider only those terms in the loop integral that do not depend on the external momentum.





$$\Gamma_4 = -12 \left( \frac{g_t}{\sqrt{2}} \right) \frac{1}{16\pi^2 \langle \phi \rangle^2} \left[ m_h^2 \ln \frac{\Lambda^2}{\mu^2} \right], \quad (25)$$

$$\Gamma_5 = - \left( \frac{g_t}{\sqrt{2}} \right) \frac{1}{16\pi^2 \langle \phi \rangle^2} \left[ -12\Lambda^2 + (12m_\phi^2 - 20m_t^2) \ln \frac{\Lambda^2}{\mu^2} \right], \quad (26)$$

where  $\mu$  is the renormalization scale. The wave function renormalization constant  $Z_t$  of the top quark arise from the Feynman diagrams shown in Figure 2b

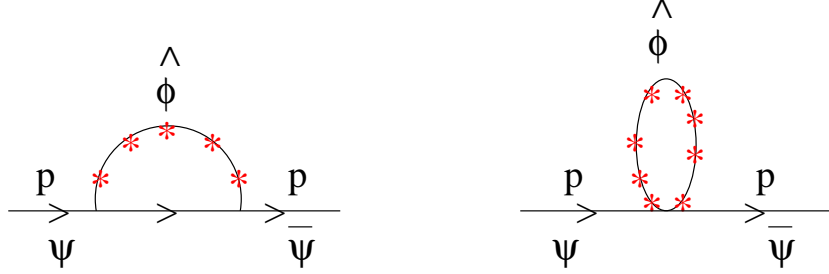


Figure 2b: *Feynman diagrams giving rise to  $Z_t$ .*

Considering the terms proportional to  $\not{p}$  of Figure 2b, it can be shown that

$$Z_t = 1 + \frac{1}{16\pi^2 \langle \phi \rangle^2} \left[ \frac{39}{8} \Lambda^2 - 6m_\phi^2 \ln \frac{\Lambda^2}{\mu^2} + \frac{13}{4} m_t^2 \ln \frac{\Lambda^2}{\mu^2} \right]. \quad (27)$$

Following the above vertex and wave function renormalization constants, it can be shown that the radion contribution  $g_t(\mu)$  to the renormalized Yukawa coupling is given by

$$g_t(\mu) = \frac{g_t}{16\pi^2 \langle \phi \rangle^2} \left[ \frac{9}{8} \Lambda^2 - 2m_\phi^2 \ln \frac{\Lambda^2}{\mu^2} - \frac{31}{2} m_t^2 \ln \frac{\Lambda^2}{\mu^2} - \frac{9}{4} m_h^2 \ln \frac{\Lambda^2}{\mu^2} \right]. \quad (28)$$

The complete beta function for  $g_t$  in the presence of radion fluctuations one finds as [52, 53]

$$\beta(g_t(\mu)) = \beta_{SM}(g_t(\mu)) + \frac{g_t}{16\pi^2 \langle \phi \rangle^2} \left[ 4m_\phi^2 + \frac{31}{2} g_t^2 v^2 + 9\lambda v^2 \right], \quad (29)$$

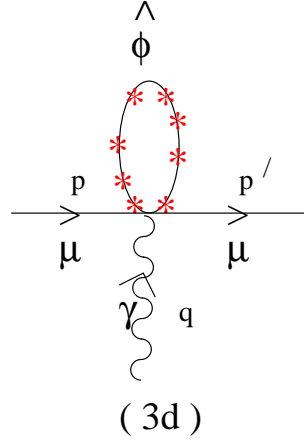
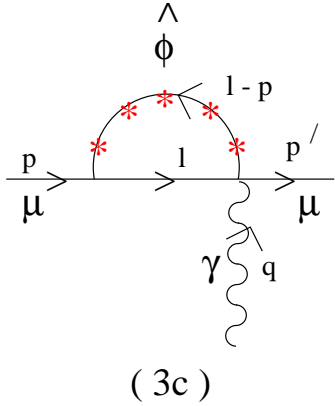
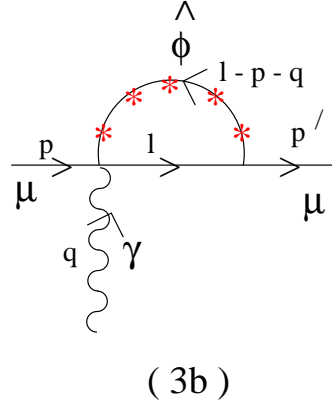
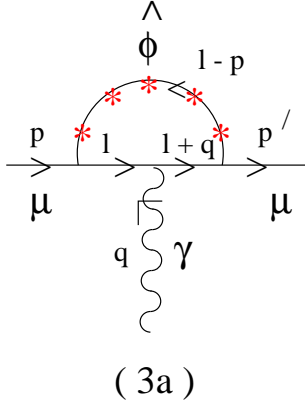
where

$$\beta_{SM}(g_t(\mu)) = \frac{g_t}{16\pi^2} \left[ \frac{9}{2} g_t^2 - 8g_3^2 - \frac{9}{4} g_2^2 - \frac{17}{12} g_1^2 \right] \quad (30)$$

is the pure SM part [54].

## 2.3 Radion contribution to muon anomaly

We now find the radion contribution to the muon anomaly. The possible Feynman diagrams contributing to muon anomaly are shown in Figures 3(a, b, c, d):



Figures 3[a,b,c,d]: *Feynman diagrams contributing to muon anomalous magnetic moment.*

We regularize these diagrams by using the cut-off regularization technique with the ultra-violet cut-off as  $\Lambda$ . A glimpse of the main results are presented below

For Figure 3(a):

$$-ie\Lambda_{1\mu}(p, q, p') = \frac{9e}{2\langle\phi\rangle^2} \int_0^1 \int_0^1 xdx dy \int \frac{d^4l}{(2\pi)^4} \frac{[\not{l}_0 + 2\not{p}' - \frac{8}{3}m][\not{l}_0 + \not{p}' + m]\gamma_\mu[\not{l}_0 + \not{p}' + m][\not{l}_0 + 2\not{p} - \frac{8}{3}m]}{[l^2 - R_1^2]^3} \quad (31)$$

which gives

$$\begin{aligned}\Lambda_{1\mu} = & \frac{9i}{2\langle\phi\rangle^2} \int_0^1 x dx \int_0^1 dy \left[ \frac{2}{3} m_\mu (2xy - 1) \right] \left[ \frac{i}{16\pi^2} \text{Log}[\Lambda^2/R_1^2] - \frac{3i}{32\pi^2} \right] (p + p')_\mu \\ & + \frac{9i}{2\langle\phi\rangle^2} \int_0^1 x dx \int_0^1 dy \left[ \frac{2}{3} m_\mu^3 A \right] \left[ -\frac{i}{32\pi^2 R^2} \right] (p + p')_\mu, \quad (32)\end{aligned}$$

where  $l_0 = l - pxy - p'x(1 - y)$ ,  $R_1^2 = m_\mu^2 x^2 + m_\phi^2(1 - x)$  and  $A = 2x^3y + \frac{4}{3}x^2y - x^2 - \frac{8}{3}xy$ .

For Figure 3(b)

$$\begin{aligned}-ie\Lambda_{2\mu}(p, q, p') = & -\frac{9e}{2\langle\phi\rangle^2} \int_0^1 dx \int \frac{d^4l}{(2\pi)^4} \frac{[l'_1 + 2p' - \frac{8}{3}m][l'_1 + p' + m]\gamma_\mu}{[l^2 - R_2^2]^2} \\ = & -\frac{9e}{2\langle\phi\rangle^2} \int_0^1 dx \int \frac{d^4l}{(2\pi)^4} \frac{[l^2 + m^2x^2 - 2xm^2 + \frac{2}{3}xm - \frac{4}{3}m^2]\gamma_\mu}{[l^2 - R_2^2]}, \quad (33)\end{aligned}$$

where  $R_2^2 = m_\mu^2 x^2 + m_\phi^2(1 - x)$  and  $l'_1 = l - xp'$ .

Similarly for Figure 3(c)

$$\begin{aligned}-ie\Lambda_{3\mu}(p, q, p') = & -\frac{9e}{2\langle\phi\rangle^2} \int_0^1 dx \int \frac{d^4l}{(2\pi)^4} \frac{\gamma_\mu [l'_2 + p' + m][l'_2 + 2p' - \frac{8}{3}m]}{[l^2 - R_3^2]^2} \\ = & -\frac{9e}{2\langle\phi\rangle^2} \int_0^1 dx \int \frac{d^4l}{(2\pi)^4} \frac{[l^2 + m^2x^2 - \frac{4}{3}m^2x - \frac{4}{3}m^2]\gamma_\mu}{[l^2 - R_3^2]}, \quad (34)\end{aligned}$$

where  $R_3^2 = m_\mu^2 x^2 + m_\phi^2(1 - x) = R_2^2 = R_1^2 = R^2$  (say) and  $l'_2 = l - xp$ .

Finally for Figure 3(d), we find

$$-ie\Lambda_{4\mu}(p, q, p') = \frac{3e}{\langle\phi\rangle^2} \gamma_\mu \int \frac{d^4l}{(2\pi)^4} \frac{1}{l^2 - m_\phi^2}, \quad (35)$$

which gives

$$\Lambda_{4\mu} = \frac{3}{16\pi^2\langle\phi\rangle^2} \left[ \Lambda^2 - m_\phi^2 \text{Log} \left( \frac{\Lambda^2}{m_\phi^2} \right) \right] \gamma_\mu. \quad (36)$$

It is clear from the above expressions of  $\Lambda_{2\mu}, \Lambda_{3\mu}$  and  $\Lambda_{4\mu}$  that they are proportional to  $\gamma_\mu$  and hence the Feynman diagrams 3(b), 3(c) and 3(d) do not contribute to the muon anomalous magnetic moment, but they do contribute in the vertex i.e. coupling constant

renormalization. On the other hand  $\Lambda_{1\mu}$  corresponding to the Figure 3(a) is seen to be proportional to  $(p + p')_\mu$  and contribute to  $\delta a_\mu^{(new)} (= a_\mu^\phi)$ . Using the Gordon's identity

$$\bar{u}(p')\gamma_\mu u(p) = \frac{1}{2m_\mu}\bar{u}(p') [(p + p')_\mu + i\sigma_{\mu\nu}q^\nu] u(p). \quad (37)$$

and the Dirac equation of motion we finally get the radion contribution to the muon anomalous magnetic moment as [55]

$$a_\mu^\phi = \frac{36m_\mu^2}{96\pi^2\langle\phi\rangle^2} \int_0^1 x dx \int_0^1 dy (2xy - 1) \left[ \text{Log} \left( \frac{\Lambda^2}{R^2} \right) - \frac{3}{2} \right] - \frac{36m_\mu^4}{192\pi^2\langle\phi\rangle^2} \int_0^1 x dx \int_0^1 dy \frac{[2x^3y + \frac{4}{3}x^2y - x^2 - \frac{8}{3}xy]}{R^2}, \quad (38)$$

where  $R^2 = m_\mu^2 x^2 + m_\phi^2(1-x)$ ,  $m_\mu$  the muon mass. At this point it is worthwhile to note that the radion mediated muon anomaly is free from power like divergence unlike the Kaluza-Klein graviton contribution to the oblique electroweak parameters S, T and U which is plagued by uncalculable powerlike divergences [56, 57]. Now  $\Lambda$  in Eq. (38) is the ultraviolet cut-off of the theory and from a naive dimensional analysis it follows that  $\Lambda$  is equal to  $4\pi\langle\phi\rangle$  [58]. The UV limit  $\Lambda \sim \langle\phi\rangle \rightarrow \infty$  corresponds to the radion and SM decoupling limit.

### 3 Numerical Analysis

There are phenomenological limits on the  $m_\phi - \langle\phi\rangle$  parameter space. From this it follows that the lower bound on  $\langle\phi\rangle$  can range from about the electroweak symmetry breaking scale to about a TeV, while  $m_\phi$  can in principle be even lighter than  $m_W$  or heavier than the top quark. We separate our analysis in two main parts. First, we compare our radion corrected muon anomaly  $a_\mu^\phi$  with the deviation  $\delta a_\mu^{new}$  (using the BNL recent result) and obtain constraints in the  $m_\phi - \langle\phi\rangle$  plane. Second, we use the modified beta functions  $\beta(\lambda)$  and  $\beta(g_t)$  together with the anomaly constrained  $m_\phi$  and  $\langle\phi\rangle$  values to obtain lower bound on higgs mass  $m_h$ . Finally, we compare our result with the LEP2 direct bound on  $m_h$ .

### 3.1 Anomaly constraints in $m_\phi - \langle\phi\rangle$ plane

The radion contribution to the muon anomaly ( Eqn.(38)) in the limit  $\Lambda \gg m_\phi \gg m_\mu$  takes the form

$$a_\mu^{(\phi)} = \frac{36m_\mu^2}{96\pi^2\langle\phi\rangle^2} \left[ 0.12 - 0.17 \text{Log} \left( \frac{16\pi^2\langle\phi\rangle^2}{m_\phi^2} \right) - 0.26 \frac{m_\mu^2}{m_\phi^2} \right]. \quad (39)$$

From Eqs. (3) and (4) we see that the experimental result differs from the theoretical(SM) prediction by

$$\delta a_\mu^{new} = a_\mu^{(expt)} - a_\mu^{(SM)} = (28 \pm 10.5) \times 10^{-10} \quad (40)$$

which is about  $2.6 \sigma$ . The ultimate precision of the BNL collaboration is to reduce the error down to  $4.0 \times 10^{-10}$ . We will consider the BNL recent result for our analysis and make some comments regarding the ultimate precision measurement.

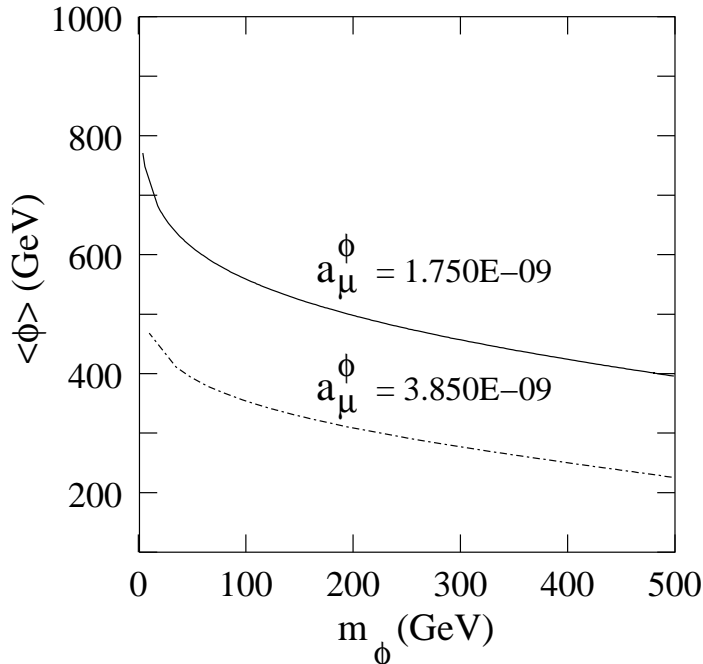


Figure 4. *Muon anomaly constraints on  $m_\phi$  and  $\langle\phi\rangle$ . For any curve the allowed region lies at and above the curve.*

In Figure 4 we draw the contour plots in  $m_\phi - \langle\phi\rangle$  plane corresponding to of  $a_\mu^\phi [= \delta a_\mu^{new}] = 1.75 \times 10^{-9}$  and  $3.85 \times 10^{-9}$ . The following things are to be noted:

- For a given  $m_\phi$  the lower bound on  $\langle\phi\rangle$  increases with the decrease in  $a_\mu^\phi$ . As an example for  $m_\phi = 100$  GeV when  $a_\mu^\phi$  varies from  $3.850 \times 10^{-9}$  to  $1.750 \times 10^{-9}$ ,  $\langle\phi\rangle$  changes from 354 GeV to 559 GeV.
- For a given  $a_\mu^\phi$  the lower bound on  $\langle\phi\rangle$  decreases with the increase in  $m_\phi$ .
- For any curve the region at and above the curve is allowed.
- Elaborating Figure 4, we find that the BNL ultimate(projected) precision measurement suggests the lower bound on  $\langle\phi\rangle$  larger than 400 GeV for a heavy radion (for  $m_\phi = 500$  GeV), while  $\langle\phi\rangle > 1000$  GeV for a lighter one i.e.  $m_\phi = 100$  GeV.

### 3.2 Lower bound on higgs mass $m_h$

To obtain bound on  $m_h$  rewrite  $\beta(\lambda)$  and  $\beta(g_t)$  as

$$\beta(\lambda) = \frac{d\lambda}{dt} = \mu \frac{d\lambda}{d\mu} = \frac{1}{8\pi^2} \left[ 9\lambda^2 + \frac{402\lambda^2 v^2}{\langle\phi\rangle^2} + \frac{144\lambda^2 v^4}{\langle\phi\rangle^4} + \frac{5\lambda m_\phi^2}{\langle\phi\rangle^2} + \lambda \left( 6g_t^2 - \frac{9}{2}g_2^2 - \frac{3}{2}g_1^2 \right) - 6g_t^4 \right] + \frac{1}{8\pi^2} \left[ \frac{3}{4} \left( g_t^4 + \frac{1}{2}(g_2^2 + g_1^2)^2 \right) \right] \quad (14)$$

and

$$\beta(g_t) = \frac{dg_t}{dt} = \beta_{SM}(g_t) + \frac{g_t}{16\pi^2 \langle\phi\rangle^2} \left[ 4m_\phi^2 + \frac{31}{2}g_t^2 v^2 + 9\lambda v^2 \right], \quad (29)$$

where

$$\beta_{SM}(g_t) = \frac{g_t}{16\pi^2} \left[ \frac{9}{2}g_t^2 - 8g_3^2 - \frac{9}{4}g_2^2 - \frac{17}{12}g_1^2 \right].$$

In above  $v(= 247$  GeV) is the electro-weak vev,  $g_2$  and  $g_1$  are the  $SU(2)_L$  and  $U(1)_Y$  coupling constants and  $t = \log(\frac{\mu}{\mu_0})$  with  $\mu$ , the renormalization scale and  $\mu_0$ , a reference scale (in our case is chosen as  $m_Z$ ). Note that the terms which arise as corrections due to radion in  $\beta(\lambda)$  and  $\beta(g_t)$  goes in powers of  $1/\langle\phi\rangle$ . Rest are the SM terms.

We combine the anomaly constrained  $m_\phi$  and  $\langle\phi\rangle$  with the above modified  $\beta(\lambda)$  and  $\beta(g_t)$  to obtain bound on  $m_h$ . For this we consider the following steps:

1. In Figure 4 we have seen that for a given  $a_\mu^\phi$  the lower bound on  $\langle\phi\rangle$  decreases with the increase of  $m_\phi$ . Although for a given curve the region at and above the curve is allowed, we will choose the points on the curves.

2. Now we find the higgs quartic coupling  $\lambda(\mu = 115)$  (GeV) by solving the beta function  $\beta(\lambda)$  ( Eq. (14)) for the following two initial value (required while running them from top to bottom):

(i)  $\lambda(\Lambda = 4\pi\langle\phi\rangle) = 3.54491$ , non-perturbative and

(ii)  $\lambda(\Lambda = 4\pi\langle\phi\rangle) = 0.313$  i.e. perturbative.

Note that in Eqs. (14) and (29) the coupling constants  $g_1$ ,  $g_2$  and  $g_3$  are renormalized coupling constants. Their relevant beta functions(to one loop order) are given by

$$\beta(g_1) = \frac{41}{96\pi^2} g_1^3, \quad (41)$$

$$\beta(g_2) = -\frac{19}{96\pi^2} g_2^3, \quad (42)$$

and

$$\beta(g_3) = -\frac{7}{16\pi^2} g_3^3. \quad (43)$$

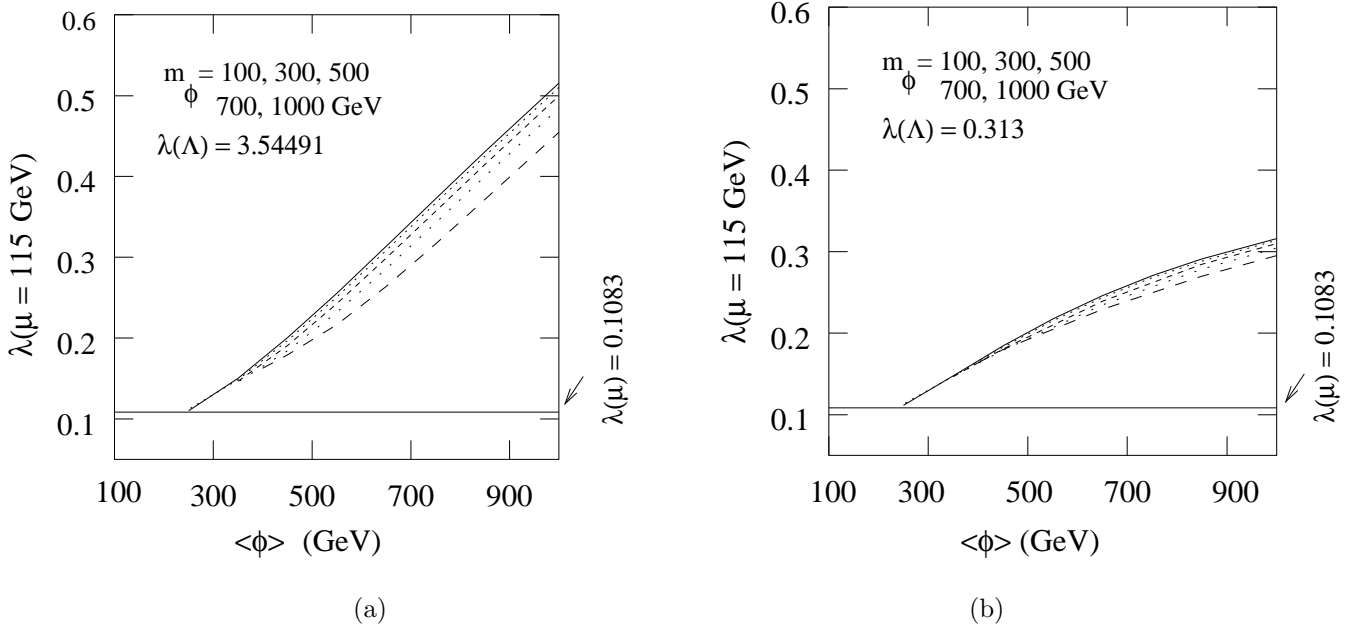
In solving the above renormalization group(RG) equations, we use the following inputs  $g_t(\mu = m_Z) = \frac{\sqrt{2}m_t}{v} = 1.001$ ,  $g_2(m_Z) = \frac{e}{\sin\theta_w} = 0.644$  and  $g_1(m_Z) = \frac{e}{\cos\theta_w} = 0.356$ . Using the above RG equations we next run all the coupling constants. First we allow them to run from  $\mu = m_Z$  to  $\mu = \Lambda$  and note their values at  $\mu = \Lambda(= 4\pi\langle\phi\rangle)$ . Then we run them from top to bottom i.e. from  $\mu = \Lambda$  to  $\mu = 115$  GeV corresponding to  $\lambda(\Lambda = 4\pi\langle\phi\rangle) = 3.54491$  and  $\lambda(\Lambda = 4\pi\langle\phi\rangle) = 0.313$  and note  $\lambda(\mu = 115$  GeV) accordingly. Plots showing  $\lambda(\mu = 115$  GeV) as a function of  $\langle\phi\rangle$ , the UV cut-off  $\Lambda (= 4\pi\langle\phi\rangle)$  are shown in Figures 5[a, b] corresponding to non-perturbative and perturbative initial conditions.

3. In Figure 5a (the non-perturbative case) we have several distinct lines corresponding to  $\lambda(\mu = 115\text{GeV})$  vs  $\langle\phi\rangle$  (GeV) plots for different  $m_\phi$  values. Now for a particular  $m_\phi$ ,  $\langle\phi\rangle$  (which is consistent with the muon anomaly constraint (see Figure 4)) is chosen from Figure 5a and the corresponding  $\lambda(\mu = 115$  GeV) is noted. A similar kind of analysis is also done for the perturbative case and accordingly Figure 5b is obtained.

4. After finding  $\lambda(\mu = 115$  GeV) corresponding to a given  $m_\phi$  and  $\langle\phi\rangle$  (which are consistent with the muon anomaly constraint), we can convert it to the higgs mass  $m_h$  by using the relation

$$m_h(\mu) = \sqrt{2\lambda(\mu)} v^2$$

respectively for the perturbative and non-perturbative cases.



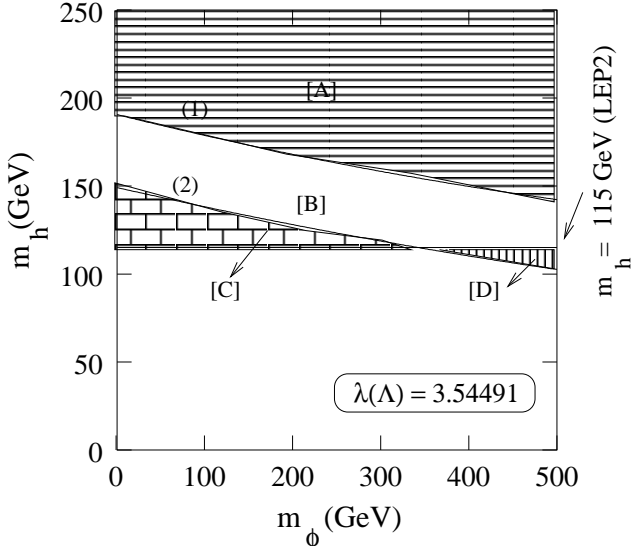
Figures 5[a, b]. Plots showing  $\lambda(\mu = 115 \text{ GeV})$  as a function of  $\langle \phi \rangle$  with  $\lambda(\Lambda) = 3.54491$  and  $= 0.313$  for different  $m_\phi$  values.

5. We next plot the higgs mass  $m_h$  as a function of  $m_\phi$  for  $a_\mu^\phi = 1.750 \times 10^{-9}$  and  $3.850 \times 10^{-9}$  respectively for  $\lambda(\Lambda) = 3.5449$  and  $\lambda(\Lambda) = 0.313$  in either case and they are shown in Figures 5c and 5d. The horizontal line (in both figures) corresponds to the LEP2 lower bound on  $m_h$  which is about 115 GeV (See [48] for LEP2 direct search of higgs boson).

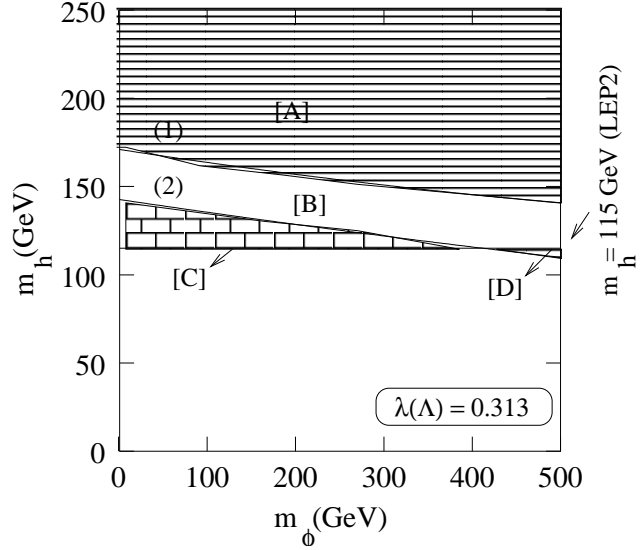
6. In Figure 5c the region **A** is allowed both by the LEP2 direct search and the muon anomaly  $\delta a_\mu^{(new)} = a_\mu^\phi = 1.750 \times 10^{-9}$  and it gives a lower bound on  $m_h$  which varies from 190 GeV to 142 GeV for  $m_\phi$  ranges from 1 GeV to 500 GeV. It is to be noted that the lower bound on  $m_h$  corresponding to  $a_\mu^\phi = 1.750 \times 10^{-9}$  is all throughout greater than the LEP2 bound. Similarly in Figure 5d, corresponding to  $a_\mu^\phi = 1.750 \times 10^{-9}$  we see that the lower bound on  $m_h$  varies from 170 GeV to 141 GeV for  $m_\phi$  ranges from 1 GeV to 500 GeV.

7. The region **B** in Figures 6[c,d] is allowed both by the direct LEP2 search and  $a_\mu^\phi = 3.850 \times 10^{-9}$ , but forbidden by  $a_\mu^\phi = 1.750 \times 10^{-9}$ . Interesting bound on  $m_h$  follows from this region. We find a lower bound of about 115 GeV on  $m_h$  which is compatible with the LEP2 bound. We also obtain the upper bounds on  $m_h$  depending on whether  $\lambda(\Lambda)$  is non-perturbative or perturbative. They are about 142 GeV and 141 GeV corresponding to  $m_\phi = 500$  GeV respectively for  $\lambda(\Lambda) = 3.5449$  and  $\lambda(\Lambda) = 0.313$ .





(c)



(d)

Figures 5[c,d]. The  $m_\phi$  vs  $m_h$  plots corresponding to  $\lambda(\Lambda) = 3.54491$  and  $= 0.313$ . The upper and the lower curve corresponds to (1)  $a_\mu^\phi = 1.750 \times 10^{-9}$  and (2)  $a_\mu^\phi = 3.850 \times 10^{-9}$ .

8. The region **C** is allowed by the direct LEP2 search but disallowed by  $\delta a_\mu^{(new)} = a_\mu^\phi$ . In addition of finding a lower bound on  $m_h$  which is compatible with the LEP2 bound, we also obtain an upper bound of about 149 GeV for the non-perturbative case and 143 GeV for the perturbative case corresponding to a very light radion (say  $m_\phi = 1 \sim 2$  GeV). Most importantly the bound on  $m_h$  corresponding to  $a_\mu^\phi = 3.850 \times 10^{-9}$  is greater than the LEP2 bound (which is about 115 GeV) if  $m_\phi < 342$  GeV for  $\lambda(\Lambda) = 3.54491$  and is  $< 412$  GeV for  $\lambda(\Lambda) = e (= 0.313)$ . Translating this to  $\langle \phi \rangle$  one finds the lower bounds on  $\langle \phi \rangle$  as 266 GeV and 247 GeV corresponding to  $a_\mu^\phi = 3.850 \times 10^{-9}$ .

9. Finally the region **D** in Figures 5c and 5d which is ruled out by direct LEP2 search, allowed by  $\delta a_\mu = 3.850 \times 10^{-9}$ . Since it is forbidden by LEP2 data, we do not consider this region any further.

## 4 Summary and Conclusion:

The model of warped spatial dimension (the Randall-Sundrum model) with a light stabilized radion possesses several interesting phenomenological features. We explore one such feature

in the present work. We calculate the radion mediated muon anomaly  $a_\mu^\phi$  and use the BNL muon anomaly data to constrain  $m_\phi$  and  $\langle\phi\rangle$ , the two free parameters of this model. The beta functions  $\beta(\lambda)$ ,  $\beta(g_t)$  for the higgs quartic coupling  $\lambda$  and the higgs-top Yukawa coupling  $g_t$  gets modified in the presence of radion and we determine these modified functions. Using these modified beta functions and the anomaly constrained  $m_\phi$  and  $\langle\phi\rangle$  we obtain lower bound on higgs mass  $m_h$ . For  $a_\mu^\phi = 3.850 \times 10^{-9}$ , we find that the bound on  $m_h$  is greater than the LEP2 bound if  $m_\phi < 342$  GeV for  $\lambda(\Lambda) = 3.54491$  and is  $< 412$  GeV for  $\lambda(\Lambda) = 0.313$ . Translating this to  $\langle\phi\rangle$  one finds lower bound of 266 GeV and 247 GeV for  $\lambda(\Lambda) = 3.54491$  and  $\lambda(\Lambda) = 0.313$ , respectively. The bound on  $m_h$  corresponding to  $a_\mu^\phi = 1.750 \times 10^{-9}$  is found to be greater than the LEP2 bound for a wide range of  $m_\phi$  both for perturbative and non-perturbative values of  $\lambda(\Lambda)$ .

## Acknowledgement:

I would like to thank late Prof. Uma Mahanta of HRI who taught me the Randall-Sundrum model and to Prof. Biswarup Mukhopadhyaya of HRI for his useful suggestions and comments while reading the manuscript. Special thanks to Prof. Saurabh Rindani for providing me a nice stay at the PRL where this work is finally completed.

## References

- [1] N. Arkani-Hamed, S. Dimopoulos and G. Dvali, *Phys. Lett.* **B429** , 263 (1998).
- [2] I. Antoniadis, N. Arkani-Hamed and G. Dvali, *Phys. Lett.* **B463**, 257 (1998).
- [3] L. Randall and R. Sundrum, *Phys. Rev. Lett.* **83**, 3370 (1999).
- [4] L. Randall and R. Sundrum, *Phys.Rev.Lett.* **83**, 4690 (1999).
- [5] M. L. Graesser, *Phys. Rev. D* **61**, 074019 (2000).
- [6] U. Mahanta and S. Rakshit, *Phys. Lett.* **B480**, 176 (2000).
- [7] S. C. Park and H. S. Song, *Phys. Lett.* **B506**, 99 (2001).
- [8] C. S. Kim, J. D. Kim and J. Song, *Phys. Lett.* **B511**, 251 (2001).

- [9] G. F. Giudice, R. Rattazzi and J. D. Wells, *Nucl. Phys.* **B595**, 250 (2001).
- [10] W. D. Goldberger and M. B. Wise, *Phys. Lett.* **B475** 275-279 (2000).
- [11] W. D. Goldberger and I. Z. Rothstein, *Phys. Lett.* **B491** 339 (2000).
- [12] W. D. Goldberger and M. B. Wise, *Phys. Rev. Lett.* **83** 4922 (1999).
- [13] W. D. Goldberger and M. B. Wise, *Phys. Rev.* **D 60** 107505 (1999).
- [14] K. Cheung, *Phys. Rev.* **D63** 056007 (2001).
- [15] C. Csaki, M. Graesser, L. Randall and J. Terning, *Phys. Rev.* **D62** 045015 (2000).
- [16] U. Mahanta and A. Datta, *Phys. Lett.* **B483** 196 (2000).
- [17] S. Bae, P. Ko, H. Lee and J. Lee, *Phys. Lett.* **B487** 299 (2000).
- [18] P. K. Das and U. Mahanta, *Phys. Lett.* **528** 253 (2002).
- [19] P. K. Das and U. Mahanta, *Mod. Phys. Lett.* **A**, 127 (2004).
- [20] M. Chaichian, A. Datta, K. Huitu and Z. Yu, *Phys. Lett.* **B524** 161 (2002).
- [21] G. W. Bennett et. al. [Muon g-2 collaboration], hep-ex/0208001.
- [22] H. N. Brown et. al. *Phys. Rev. Lett.* **86**, 2227 (2001).
- [23] D. H. Hertzog, hep-ex/0202024.
- [24] M. Knecht and A. Nyffeler, *Phys. Rev.* **D65** 073034 (2002).
- [25] M. Knecht, A. Nyffeler, M. Perrotet and E. de Rafael, *Phys. Rev. Lett.* **88**, 071802 (2002).
- [26] M. Hayakawa and T. Kinoshita, hep-ph/0112102.
- [27] I. Blokland, A. Czarnecki and K. Melnikov, *Phys. Rev. Lett.* **88**, 071803 (2002).
- [28] A. Czarnecki and W.J. Marciano, *Phys. Rev.* **D64**, 013014 (2001).

- [29] K. Lane, hep-ph/0102131.
- [30] L. Everett, G. Kane, S. Rigolin and L. Wang, *Phys. Rev. Lett.* **86**, 3484 (2001).
- [31] J.L. Feng and K.T. Matchev, *Phys. Rev. Lett.* **86**, 3480 (2001).
- [32] E.A. Baltz and P. Gondolo, *Phys. Rev. Lett.* **86**, 5004 (2001).
- [33] U. Chattopdhyay and P. Nath, *Phys. Rev. Lett.* **86**, 5854 (2001).
- [34] U. Mahanta, *Phys. Lett.* **B515**, 111 (2001).
- [35] D. Chakraverty, D. Choudhury and A. Datta, *Phys. Lett.* **B506**, 103 (2001).
- [36] D. Choudhury, B. Mukhopadhyaya and S. Rakshit, *Phys. Lett.* **B507**, 219 (2001).
- [37] R. Barbieri and L. Maiani, *Phys. Lett.* **B117** , 203 (1982).
- [38] D.A. Kosower, L.M. Krauss and N. Sakai, *Phys. Lett.* **B133**, 305 (1983).
- [39] R. Arnowitt, A.H. Chamseddine and P. Nath, *Z. Physik* **C26**,407 (1984).
- [40] J.L. Lopez, D.V. Nanopoulos and X. Wang, *Phys. Rev.* **D49** , 366 (1994).
- [41] C. Arzt, M.B. Einhorn and J. Wudka, *Phys. Rev.* **D49** , 1370 (1994).
- [42] U. Chattopadhyay and P. Nath, *Phys. Rev.* **D53** , 1648 (1996).
- [43] M. Carena, G.F. Giudice and C.E. Wagner, *Phys. Lett.* **B390**, 234 (1997).
- [44] P. Nath and M. Yamaguchi, *Phys. Rev.* **D60** , 116006 (1999).
- [45] R. Casadio, A. Gruppuso and G. Venturi, *Phys. Lett.* **B495** , 378 (2000).
- [46] H. Davoudiasl, J.L. Hewett and T.G. Rizzo, *Phys. Lett.* **B493** , 135 (2000).
- [47] A. Czarnecki and W.J. Marciano, hep-ph/0010194 and references therein.
- [48] T. Junk, The LEP Higgs Working Group at LEP Fest October 10th, 2002.
- [49] P. K. Das, S. K. Rai and S. Raychaudhuri, *Phys. Lett.* **B618**, 221 (2005).

- [50] J. C. Collins, A. Duncan and S. D. Joglekar, *Phys. Rev. D* **16**, 438 (1977).
- [51] P. K. Das and Uma Mahanta, *Phys.Lett.* **B520**, 307 (2001).
- [52] P. K. Das and U. Mahanta, hep-ph/011030.
- [53] P. K. Das and U. Mahanta, *Int.J.Mod.Phys.* **A20**, 1089 (2005).
- [54] W. Bardeen, C. Hill and M. Lindner, *Phys. Rev.* **D41**, 1647 (1990).
- [55] P. K. Das and Uma Mahanta, *Nucl. Phys.* **B644**, 395-400 (2002).
- [56] P. K. Das and S. Raychaudhuri, hep-ph/9908205.
- [57] T. Han, D. Marfatia and R. Zhang, *Phys. Rev.* **D62**, 125018 (2000).
- [58] H. Georgi and A. Manohar, *Nucl. Phys.* **B234**, 189 (1984).